

# Electric field-activated combustion synthesis of $\text{Ti}_5\text{Si}_3\text{-Nb}$ and $\text{Ti}_5\text{Si}_3\text{-ZrO}_2$ composites

I. J. SHON\*, Z. A. MUNIR

*Department of Chemical Engineering and Materials Science, University of California, Davis, CA 95616, USA*

The field-activated combustion synthesis of the composites  $\text{Ti}_5\text{Si}_3 - x\text{Nb}$  ( $0 \leq x \leq 0.35$ ) and  $\text{Ti}_5\text{Si}_3 - y\text{ZrO}_2$  ( $0 \leq y \leq 0.3$ ) has been investigated. Composites with  $x \geq 0.35$  and  $y \geq 0.2$  can only be synthesized in the presence of an electric field. Although in the absence of a field the systems with  $x = 0.35$ ,  $y = 0.2$  and  $y = 0.3$  can sustain a non-steady combustion wave, the reaction is not complete. An unstable wave propagates to the middle of the sample and then becomes extinguished. The wave velocity of the  $\text{Ti}_5\text{Si}_3\text{-Nb}$  and  $\text{Ti}_5\text{Si}_3\text{-ZrO}_2$  composites increased slightly with the application of a field.

## 1. Introduction

Recent interest in titanium silicide,  $\text{Ti}_5\text{Si}_3$ , has focused on its potential for high temperature applications. Its high melting temperature (2403 K), good strength at high temperature, good creep resistance, low density ( $4.32 \text{ g cm}^{-3}$ ), and high oxidation resistance are attractive features for such applications [1–3]. However, as in the case of many similar compounds, its low fracture toughness below the ductile–brittle transition temperature ( $2.5 \text{ MPa m}^{1/2}$ ) is a significant limitation for its use [4]. To alleviate this problem a second phase is typically added to form  $\text{Ti}_5\text{Si}_3$  composites. Niobium and zirconia are examples of the added phases.

Niobium is attractive as an additive because of a high melting temperature (2745 K) and a thermal expansion coefficient ( $7.3 \times 10^{-6} \text{ K}^{-1}$ ) nearly equal to that of  $\text{Ti}_5\text{Si}_3$  ( $7.1 \times 10^{-6} \text{ K}^{-1}$ ) [5]. The principle toughening mechanism in composites reinforced with Nb is assumed to be plastic dissipation in the ductile reinforcements bridging the crack face [6]. In the case of composites reinforced with zirconia, the martensitic transformation from metastable tetragonal zirconia particles to monoclinic zirconia either spontaneously on cooling or in the vicinity of crack-tip stress fields provides the improvement in the mechanical properties [7].

The silicide  $\text{Ti}_5\text{Si}_3$  can be successfully prepared by self-propagating high-temperature synthesis. However, depending on the amount of the added phase the direct synthesis of  $\text{Ti}_5\text{Si}_3$  composites may not be possible by this method. To synthesize similar composites, a new method was recently developed [10]. It utilizes electric fields to activate the self-propagating high-temperature synthesis (SHS) process. With the imposition of an external electric field across the

sample, ignition results in the initiation and propagation of a combustion wave in reactant systems which normally cannot sustain such a wave. This method, referred to as the field-activated combustion synthesis, FACS, has been used to synthesize a variety of materials including  $\text{MoSi}_2\text{-Nb}$ ,  $\text{MoSi}_2\text{-ZrO}_2$  composites [11],  $\text{MoSi}_2\text{-SiC}$  composites [12], SiC [13] and others [10]. In this paper we report on the field-activated synthesis of  $\text{Ti}_5\text{Si}_3\text{-xNb}$  and  $\text{Ti}_5\text{Si}_3\text{-yZrO}_2$  composites.

## 2. Experimental procedures

The materials used in this work were 99.7% pure titanium powder, 99.5% pure silicon powder, 99.8% pure niobium powder, and 99% pure zirconia powder. The first was obtained from the Atlantic Equipment Engineers (Bergen Field, NJ) and the last three were obtained from Alfa Products, (Ward Hill, MA). The powders had a sieve classification of  $-325$  ( $<44 \mu\text{m}$ ). Two different sets of experiments using elemental powders of Ti, Si, and the additives were carried out for this study. The first set focused on the synthesis of  $\text{Ti}_5\text{Si}_3 + x \text{ vol } \% \text{ Nb}$  with  $x = 0, 10, 20, 30, 35$ . In the second set, the synthesis of  $\text{Ti}_5\text{Si}_3 + y \text{ vol } \% \text{ ZrO}_2$  with  $y = 10, 20, 30$  was the objective. Tetragonally-shaped reactant pellets with dimensions of  $10 \times 15 \times 13 \text{ mm}$  were made in a two-plunger steel die by uniaxial pressing. Typical pelleting pressure and sample weight values were about 150 MPa and 5 g, respectively. The relative green density of the pellets was maintained at about 55% for all samples in both sets of experiments. The pellets were combusted inside a stainless steel combustion chamber under 1 atm ( $1.013 \times 10^5 \text{ Pa}$ ) pressure of Ar gas. The chamber has two quartz windows to allow for the simultaneous

\* Visiting Professor, Permanent address: Department of Materials Engineering, Chonbuk National University, Chonbuk, Republic of Korea, 560-756.

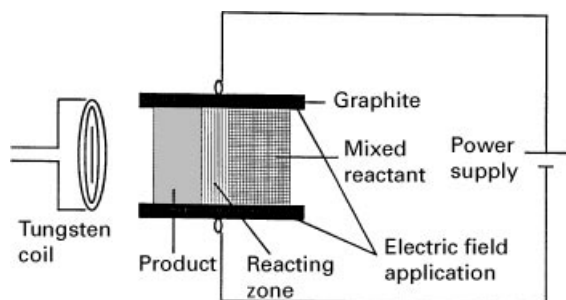


Figure 1 Schematic of the field-activated combustion apparatus.

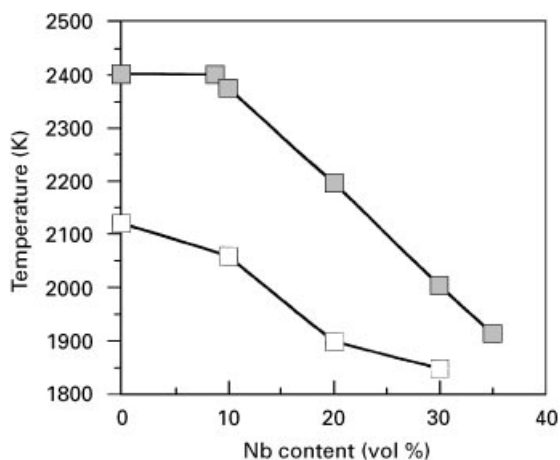


Figure 2 The variation of the combustion temperature of the  $\text{Ti}_5\text{Si}_3\text{-Nb}$  composites with the concentration of Nb. Key: (□) experimental data and (■) calculated values.

recording of the combustion wave velocity and the combustion temperature,  $T_c$ . Temperatures were also determined from the output of a W-5% Re/W-26% Re thermocouple placed inside a small hole drilled in the side of the specimen. The combustion wave velocity was determined by timing the period of the propagation from one side of the specimen to the other using a video camera with a time-code generator. The electric field was applied in a perpendicular direction to the wave propagation using two graphite electrodes, as shown schematically in Fig. 1. The distance between electrodes is 13 mm and thus field values can be calculated by dividing the voltages by this quantity. Current and voltage measurements were made simultaneously during wave propagation. Analysis of the products was made through X-ray diffraction, and microstructural and chemical analyses were made by scanning electron microscopy equipped with an energy dispersive spectrometer (EDX).

TABLE I Thermodynamic data for  $\text{Ti}_5\text{Si}_3$ , Nb, and  $\text{ZrO}_2$

Material	Heat capacity of solid ( $\text{J mol}^{-1}\text{K}^{-1}$ )				$C_p$ of liquid ( $\text{J mol}^{-1}\text{K}^{-1}$ )	$\alpha \rightarrow \beta$ transition temperature (K)	Enthalpy $\Delta H_{\alpha \rightarrow \beta}$ transition ( $\text{J mol}^{-1}$ )	Melting point (K)	Latent heat, $\Delta H_m$ ( $\text{KJ mol}^{-1}$ )	Formation enthalpy $H$ ( $\text{KJ mol}^{-1}$ ) at 298
	A	B	C	D						
$\text{Ti}_5\text{Si}_3$	196.439	44.769	-2.008	0				2403	178.99	579.484
Nb	27.782	-3.837	-0.255	3.602	41.781			2745	26.368	0
$\text{ZrO}_2, \alpha$	70.120	7.021	-1.423	0		1478	6861	2950	87.03	1101.0
$\beta$	78.601									

### 3. Results and discussion

Calculations of the adiabatic combustion temperature and its dependence on the Nb and  $\text{ZrO}_2$  content were made using the thermodynamic data presented in Table I. Comparisons between the measured and calculated adiabatic combustion temperatures are shown in Figs 2 and 3 for the  $\text{Ti}_5\text{Si}_3\text{-Nb}$  and  $\text{Ti}_5\text{Si}_3\text{-ZrO}_2$  systems, respectively. Because of heat loss in real experiments, the measured values are considerably lower than the calculated ones. Without Nb or  $\text{ZrO}_2$  additives, the combustion synthesis solely produced the  $\text{Ti}_5\text{Si}_3$  phase, as can be seen from the X-ray diffraction peaks in Fig. 4a. Fig. 4b is a back-scattered electron image of this product, showing its porous nature. The effect of the field and the addition of Nb on the combustion wave velocity is shown in Fig. 5 for the  $\text{Ti}_5\text{Si}_3\text{-Nb}$  system. The wave velocity with an applied voltage of 10 V is only slightly higher than that in the absence of a field for all Nb concentrations. Also, as expected, the wave velocity decreased with increasing Nb concentration, consistent with the decrease in the combustion temperature. The line representing the field-free combustion ends at 30 vol % Nb. Samples with higher amounts of Nb cannot produce a self-sustaining wave in the absence of a field. Under an applied voltage of 10 V, SHS reactions can be extended to a composition of 35 vol % Nb. To understand the role of the field in combustion synthesis, we examined the current and voltage profiles during the synthesis of  $\text{Ti}_5\text{Si}_3$  35 vol % Nb with an applied voltage of 10 V. Without ignition, Fig. 6a, the voltage and current remain constant with time, the latter

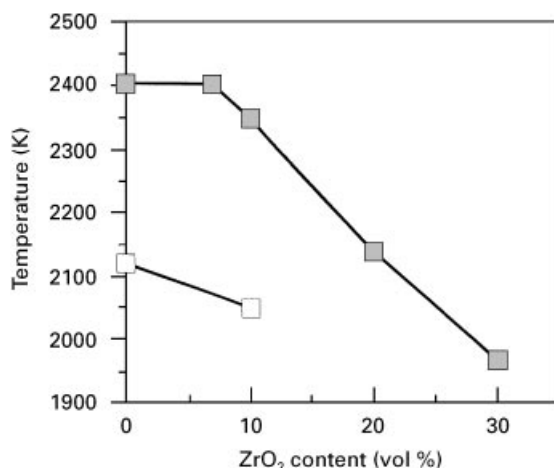


Figure 3 The variation of the combustion temperature of  $\text{Ti}_5\text{Si}_3\text{-ZrO}_2$  composites with the concentration of  $\text{ZrO}_2$ . Key: (□) experimental data and (■) calculated values.

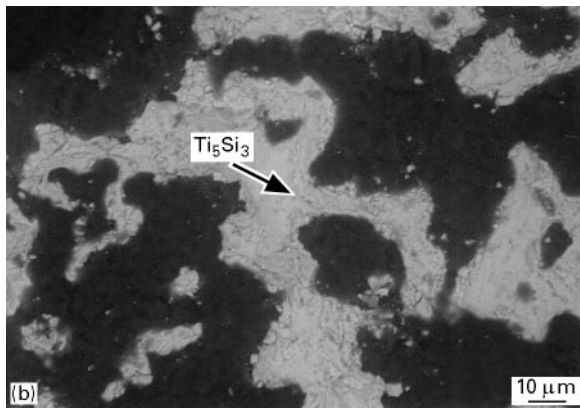
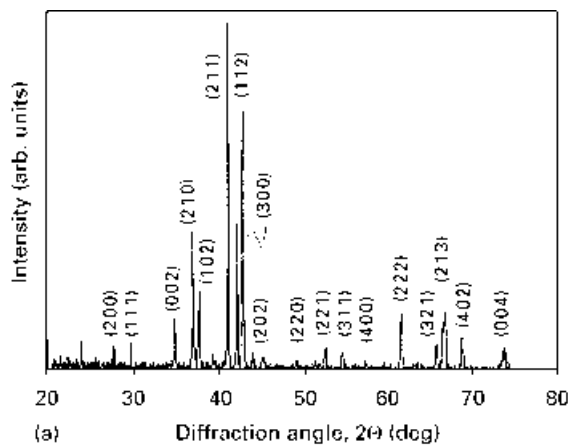


Figure 4 (a) X-ray diffraction pattern and (b) back-scattered electron image of the single-phase  $\text{Ti}_5\text{Si}_3$  product.

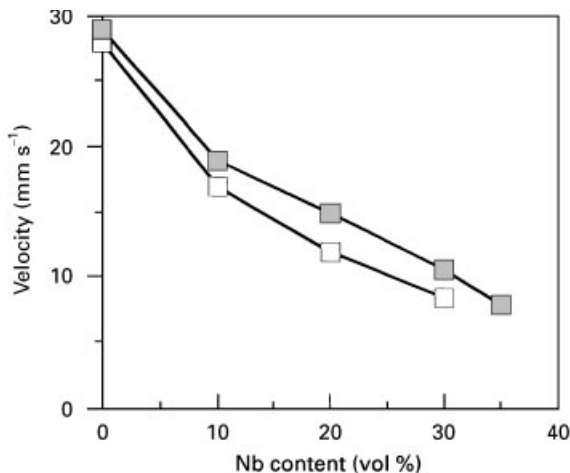


Figure 5 The variation of wave velocity of  $\text{Ti}_5\text{Si}_3$ -Nb composites with the concentration of Nb. Key: (□) 0 V and (■) 10 V.

being at an extremely low level. When an ignition source is used, however, the voltage decreased and the current increased during wave propagation, as shown in Fig. 6b. Thus the application of the field alone does not cause heating of the sample. As was proposed in a previous experimental and modelling study on SiC [13–15], the role of the field is believed to be confined to the combustion zone. The presence of a molten phase, here Si and Ti, enhances conductivity in this zone, leading to higher current densities and hence localized Joule heating. Thus, the Fourier equation for

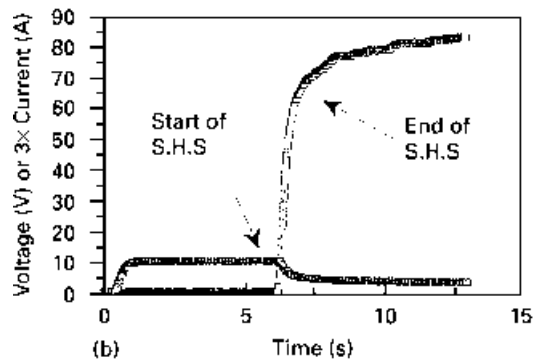
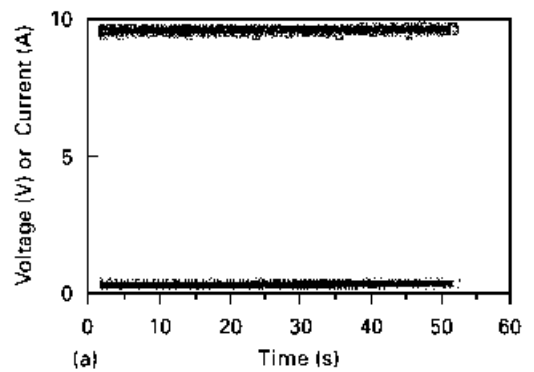


Figure 6 (■) Voltage and (□) current profiles during the synthesis of  $\text{Ti}_5\text{Si}_3$ -35 vol % Nb; (a) field application (10 V) without ignition and (b) field application (10 V) with ignition.

heat balance is modified to reflect this, i.e.,

$$\rho C_p (\partial T / \partial t) = \partial / \partial x (\kappa \partial T / \partial x) + \rho Q (\partial \eta / \partial t) + \sigma E^2 \quad (1)$$

where,  $C_p$  is the heat capacity of the product ( $\text{J g}^{-1} \text{K}^{-1}$ ),  $\rho$  is the density of the product ( $\text{g cm}^{-3}$ ),  $\kappa$  is the thermal conductivity of the product ( $\text{J cm}^{-1} \text{K}^{-1} \text{s}^{-1}$ ),  $Q$  is the heat of reaction ( $\text{J g}^{-1}$ ),  $T$  is the absolute temperature (K),  $t$  is the time (s),  $x$  is the dimension along which the wave is propagating (cm),  $\eta$  is the degree of conversion,  $\sigma$  is the electrical conductivity ( $\text{ohm}^{-1} \text{cm}^{-1}$ ) and  $E$  is the electric field ( $\text{V cm}^{-1}$ ). The heat generation terms ( $\text{J cm}^{-3} \text{s}^{-1}$ ) in the combustion zone are, therefore, chemical ( $\rho Q \partial \eta / \partial t$ ) and electrical ( $\sigma E^2$ ). It should be recalled that  $E$  is calculated on the basis of a 1.3 cm separation between the electrodes.

As indicated above, in the absence of a field a stable self-propagating wave cannot be initiated in samples with a composition corresponding to  $\text{Ti}_5\text{Si}_3$ -35 vol % Nb. Without the field an unstable wave propagated through a small portion of the sample and then stopped. Analysis of this portion of the sample showed incomplete conversion. Fig. 7(a–c) shows the diffraction peaks for the reactants (Fig. 7a), the product of combustion without the field (Fig. 7b), and, for comparison, the product when a field is applied (Fig. 7c). In Fig. 7b, peaks for  $\text{Ti}_5\text{Si}_3$  as well as Si, Ti, and Nb are present. In contrast, when a field is applied, the product is  $\text{Ti}_5\text{Si}_3$  and Nb. Back scattered electron images of the products synthesized from  $5\text{Ti} + 3\text{Si}$  with 35 vol % Nb without the electric field and with an applied voltage of 10 V are shown in Fig. 8 (a and b). Fig. 8a shows the boundary between the partially reacted and unreacted zones. In the partially reacted

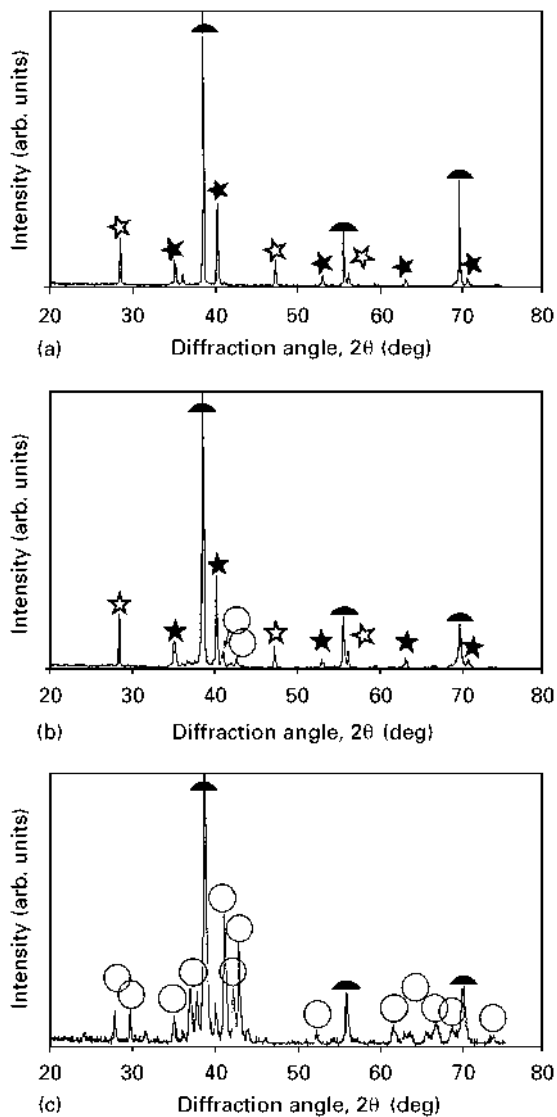


Figure 7 X-ray diffraction patterns of the synthesis 5Ti + 3Si + 35 vol % Nb; (a) reactant mixture, (b) combusted without field and (c) combusted with a 10 V field. Key: (★) Ti, (☆) Si, (▲) Nb and (○) Ti<sub>5</sub>Si<sub>3</sub>.

zone, coarse particles of Ti<sub>5</sub>Si<sub>3</sub> and relatively large regions of Nb are evident. Fig. 8b shows the microstructure of the composite prepared under the influence of a field.

Similar to the case of the Ti<sub>5</sub>Si<sub>3</sub>-Nb system, the initiation of a combustion wave and its velocity depended on the applied voltage and the concentration of ZrO<sub>2</sub> in the Ti<sub>5</sub>Si<sub>3</sub>-ZrO<sub>2</sub> samples. Fig. 9 shows that at any given ZrO<sub>2</sub> concentration (vol %) the effect of the voltage is relatively small. The voltage, however, dictated the extent of the ZrO<sub>2</sub> additive that can be added to the Ti and Si reactants and still sustain a self-sustaining reaction. Without any applied voltage, only 10 vol % ZrO<sub>2</sub> can be added. Higher limits (20 and 30 vol % ZrO<sub>2</sub>) can only be achieved when higher voltages (10 and 15 V) are applied. As before, in the absence of a field (above these limits) a non-steady state wave propagates partially through the sample. Fig. 10(a-c) shows X-ray diffraction results for the synthesis of Ti<sub>5</sub>Si<sub>3</sub>-30 vol % ZrO<sub>2</sub>. Diffraction pattern for an unreacted mixture are shown in Fig. 10a. For the product synthesized without an applied voltage, Fig. 10b, the identified phases are Ti<sub>5</sub>Si<sub>3</sub>,

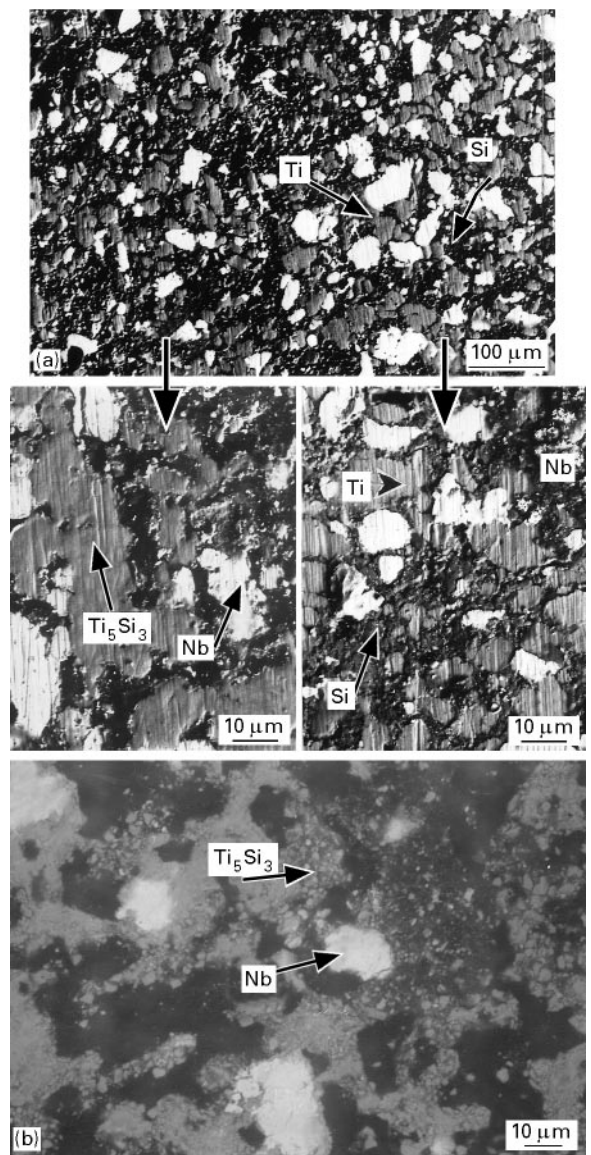


Figure 8 Back-scattered electron images of products of the 5Ti + 3Si + 35 vol % Nb, reaction; (a) synthesized without a field and (b) synthesized with a 10 V field.

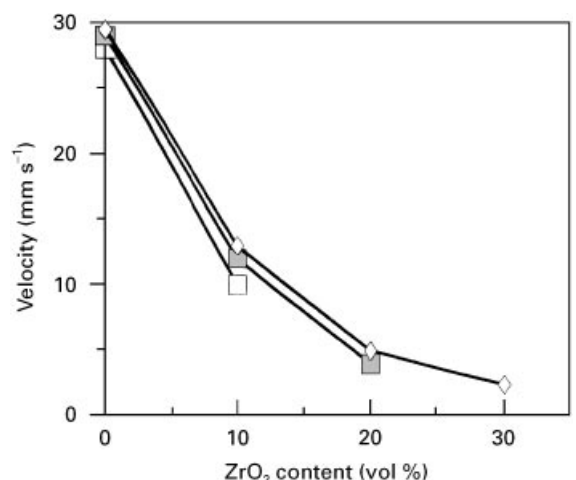


Figure 9 The variation of wave velocity of Ti<sub>5</sub>Si<sub>3</sub>-ZrO<sub>2</sub> composites with the concentration of ZrO<sub>2</sub>. Key: (□) 0 V, (■) 10 V and (◇) 15 V.

ZrO<sub>2</sub> and unreacted Ti and Si. The diffraction pattern for a sample synthesized with the 15 V (Fig. 10c), solely contains peaks for Ti<sub>5</sub>Si<sub>3</sub> and ZrO<sub>2</sub>. Fig. 11 (a and b) shows the back-scattered electron images of

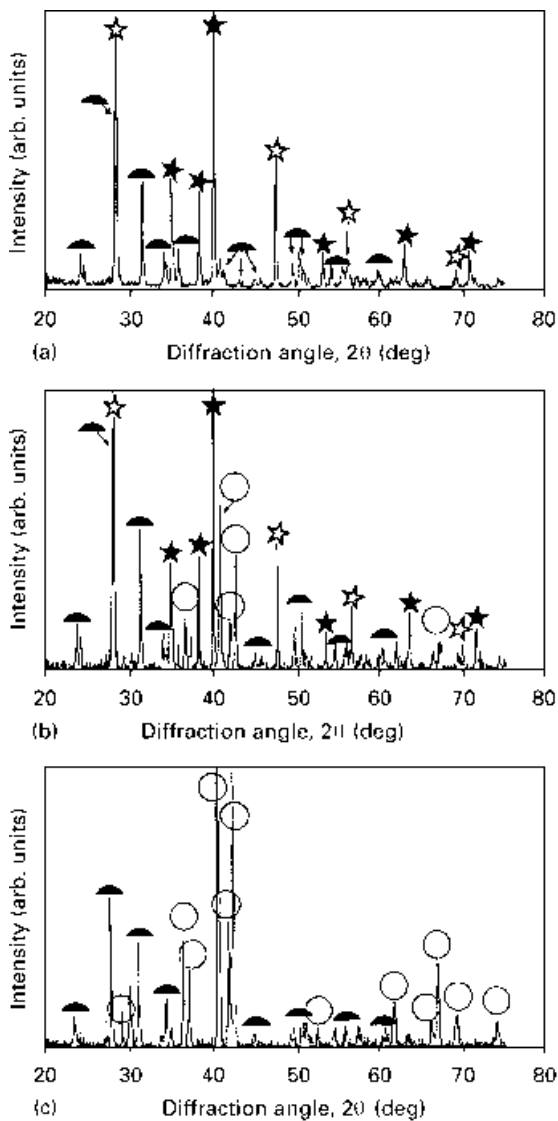


Figure 10 X-ray diffraction patterns of the synthesis  $5\text{Ti} + 3\text{Si} + 30$  vol %  $\text{ZrO}_2$ ; (a) reactant mixture, (b) combusted without field and (c) combusted with 15 V. Key: (★) Ti, (☆) Si, (▲)  $\text{ZrO}_2$  and (○)  $\text{Ti}_5\text{Si}_3$ .

products from  $5\text{Ti} + 3\text{Si}$  with 30 vol %  $\text{ZrO}_2$  reacted with and without an applied voltage of 15 V. Fig. 11a shows the boundary between the reacted and unreacted zones for the field-free case and Fig. 11b shows the microstructure of the field-assisted case. Thus, as in the case of  $\text{Ti}_5\text{Si}_3$  35 vol % Nb, the synthesis of  $\text{Ti}_5\text{Si}_3$  30 vol %  $\text{ZrO}_2$  is only partially complete when a field is not present and complete conversion to the silicide phase can only be achieved when a field is present during SHS.

#### 4. Summary

The role of an electric field in the combustion synthesis of  $\text{Ti}_5\text{Si}_3$ - $x\text{Nb}$  and  $\text{Ti}_5\text{Si}_3$ - $y\text{ZrO}_2$  composites has been investigated. Composites with  $x \geq 0.35$  and  $y \geq 0.2$  cannot be completely formed by the self-propagating combustion method without the application of an external field. For composites with Nb and  $\text{ZrO}_2$  concentrations ranging up to these limits, the imposition of field slightly increased the velocity of the combustion wave and hence the rate of conversion to the product.

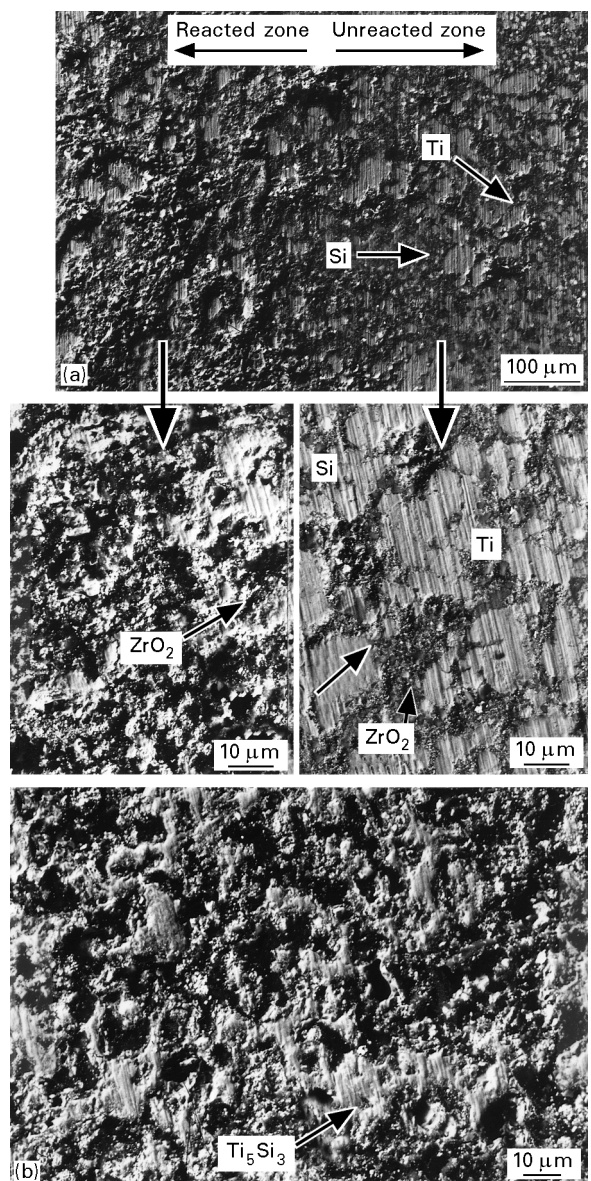


Figure 11 Back-scattered electron images of products of the  $5\text{Ti} + 3\text{Si} + 30$  vol %  $\text{ZrO}_2$  reaction; (a) synthesized without a field and (b) synthesized with a 15 V field.

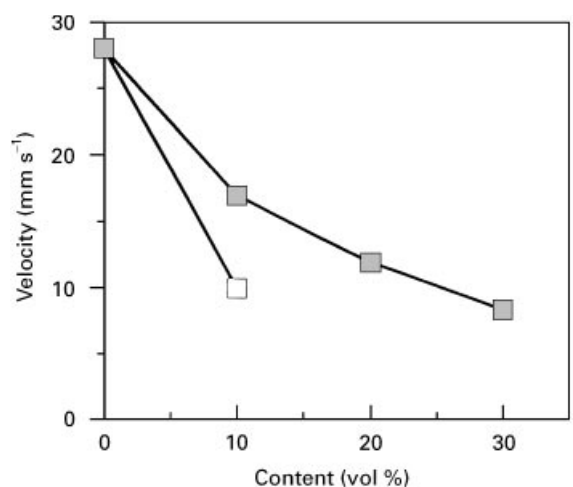


Figure 12 Comparison of the wave velocity between (■)  $\text{Ti}_5\text{Si}_3$ -Nb and (□)  $\text{Ti}_5\text{Si}_3$ - $\text{ZrO}_2$  composites during the synthesis.

## Acknowledgements

This work was supported by a grant from the National Science Foundation and the Korean Ministry of Education Research Fund for Advanced Materials.

## References

1. D. M. SHAH, D. BERCIK, D. L. ALTON and R. HETCHT, *Mater. Sci. Engng* **A155** (1992) 45.
2. P. J. MESCHTER and D. S. SCHWARTZ, *JOM* **41** (1989) 52.
3. T. SANDWICK and K. RAJAN, *J. Electronic Mater.* **19** (1990) 1193.
4. A. K. BHATTACHARYA, *J. Amer. Ceram. Soc.* **74** (1991) 2707.
5. Y. S. TOULOUKIAN, R. W. POWELL, C. Y. HO and P. G. KLEMENS, "Thermal conductivity", (IFI/Plenum, New York, 1970).
6. L. SHAW and R. ABBASCHIAN, *Acta Metall. Mater.* **42** (1994) 213.
7. J. J. PETROVIC, A. K. BHATTACHARYA, R. E. HONNELL and T. E. MITCHELL, *Mater. Sci. Engng* **A155** (1992) 259.
8. J. TRAMBUKIS and Z. A. MUNIR, *J. Amer. Ceram. Soc.* **73** (1990) 1240.
9. S. B. BHADURI, R. RADHAKRISHNAN and Z. B. QIAN, *Scripta Met. Mater.* **29** (1993) 1089.
10. Z. A. MUNIR, W. LAI and K. EWALD, US Patent 5380, 409, January (1995).
11. I. J. SHON and Z. A. MUNIR, *Mater. Sci. Engng* (in press).
12. S. GEDEVANISHVILI and Z. A. MUNIR, *Scripta Metall. Mater.* **31** (1994) 741.
13. A. FENG and Z. A. MUNIR, *J. Appl. Phys.* **76** (1994) 1927.
14. *Idem.*, *Metall. Mater. Trans.* **26B** (1995) 581.
15. *Idem.*, *ibid.*, **26B** (1995) 587.

*Received 23 February 1996  
and accepted 7 April 1997*